A BIOLOGICALLY AND GEOMETRICALLY INSPIRED APPROACH TO TARGET EXTRACTION FROM MULTIPLE-SOURCE REMOTE-SENSING IMAGERY

Lin Yan[1], Jiangye Yuan[1], Liang Cheng[1], DeLiang Wang[2], Ron Li[1],
[1]Mapping and GIS Laboratory, Department of Civil and Environmental Engineering and Geodetic Science
[2]Department of Computer Science and Engineering and Center for Cognitive Science
The Ohio State University, Columbus, OH 43210-1275
yan.351@buckeyemail.osu.edu

ABSTRACT

This paper presents the research results on the integration approach using a biologically inspired algorithm (LEGION) and a geometrically-inspired method (GAC) for target extraction from multiple-source remote-sensing imageries, specifically EO-1 Hyperion hyperspectral (30-meter resolution), and IKONOS multispectral (4-meter resolution) images. An automatic road-extraction algorithm based on LEGION (Locally Excitatory Globally Inhibitory Oscillator Networks, a neurocomputational framework for image segmentation) was developed to extract main roads from EO-1 Hyperion imagery. A region-based geometric/geodesic active contour (GAC) which adopts Euclidean distance as the basic energy metric was used to perform target extraction from both the EO-1 Hyperion and IKONOS multispectral images. The candidate targets including roads detected on the EO-1 imagery were projected onto the IKONOS imagery and used as prior knowledge for target extraction. Experimental results show that this approach reduced the computational complexity on the IKONOS imagery. Also, the use of the LEGION-based road-extraction algorithm increased the probability that major roads would be distinguished from other objects that are made of similar materials.

Key Words: LEGION, vector region-based active contour, target extraction, hyperspectral, multispectral

INTRODUCTION

Large volumes of panchromatic, multispectral and hyperspectral data have been collected from sensors onboard various satellite- and air-borne remote-sensing platforms, allowing us to derive more information than is possible from any single sensor or from sources of only broad-band spectra. The fusion of multiple-source remote-sensing data has vastly improved automatic target detection and recognition over the past decade. Meanwhile, the integration of different techniques for image processing has provided new possibilities to enhance the capabilities of target detection and recognition methodologies used on remote-sensing data. This paper presents the research on the integration of a biologically inspired method, LEGION, and a geometrically-inspired method, GAC, for target extraction from multiple-source remote-sensing imagery, specifically EO-1 Hyperion hyperspectral (30-meter resolution), and IKONOS multispectral (4-meter resolution) images.

LEGION (Locally Excitatory Globally Inhibitory Oscillator Networks) is a neurocomputational framework for image segmentation and object recognition (Wang and Terman, 1997). Taking each pixel as an oscillator, the LEGION network can rapidly achieve the segmentation of images by both synchronization in a locally coupled oscillator group (image segment) and desynchronization among different oscillator groups. LEGION has been successfully applied to the segmentation of grayscale, medical, and aerial images (Terman and Wang, 1995; Wang, 2005). In GAC (geometric/geodesic active contour) models, segmentation is achieved by evolving a signed distance function according to an energy function whose minimum is reached at the boundaries of objects in an image. GAC models have been widely used in image segmentation and object extraction because they do not impose any parametric model. They can handle topology changes, are relatively simple to implement, and have the capabilities to control the smoothness of obtained boundaries and suppress noise (Caselles et al., 1993; Chan and Vese, 2001; Niu, 2006).

This paper is organized as follows. First we discuss automatic LEGION-based road extraction. Then Vector-GAC, an extended version of the Chan-Vese model (Chan and Vese, 2001), is described. Next we present the

preliminary experimental results of combining these two algorithms for target extraction from EO-1 Hyperion and IKONOS imageries. The results are summarized in the final section.

LEGION-BASED AUTOMATIC ROAD EXTRACTION

LEGION is a biologically inspired method that allows automatic object extraction using a new structure and without any human intervention. We have developed a system that applies LEGION for automatic road extraction. This method consists of three stages: 1) image segmentation using a LEGION network; 2) medial axis extraction within each segment and selection of potential road segments; 3) grouping of potential road segments using a LEGION model with alignment-dependent connections based on extracted medial axis points.

First, an image is segmented using a LEGION algorithm. Details of the LEGION algorithm have been described at length (Wang and Terman, 1997). Based on the segmentation result, we seek to select those segments that correspond to roads. A medial axis transform is employed to achieve this goal. The medial axis of an object is defined as the loci of the centers of all the maximally inscribed circles of the object. The radius of the circle (i.e., the shortest distance to the boundary, recorded at a point of the medial axis) provides information about local thickness. The medial axis points for each segment are computed. Since roads are characterized by their narrow widths, a medial axis point is selected as a candidate if its radius is below a certain threshold.

After the selection, most of the medial axis points corresponding to roads are extracted. However, non-road points may also be included based on their small radii. In order to group road points and eliminate non-road points, we propose to use a LEGION model with alignment-dependent connections.

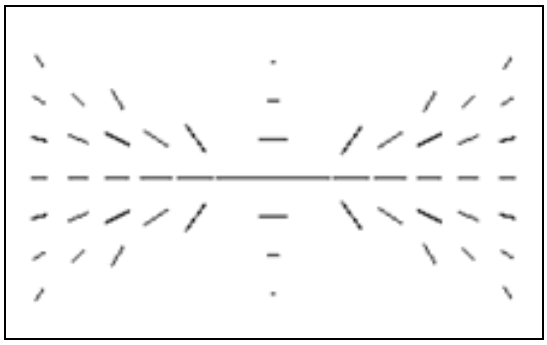

Figure 1. Connectivity pattern of a horizontally oriented cell. The cell is located at the center of the image. The orientation of each line represents the preferred orientation and the length of each line indicates connection strength.

In an image containing oriented elements, some sets of elements tend to be perceptually grouped (Yen and Finkel, 1998). It has been suggested that this perceptual effect is mediated by long-range horizontal connections within the visual cortex, which are dependent on the positions of and orientations between the elements (Yen and Finkel, 1998; Field et al., 1993). Figure 1 shows the connectivity pattern of a horizontally oriented element, which is located at the center. The orientation of other elements indicates the preferred orientation that has the strongest connection with the center element. As the actual orientation of an element deviates from the preferred one, the connection strength decreases following a Gaussian function. The connection strength also decreases as the distance between two elements increase.

Under the assumption that road segments are aligned collinearly or curvilinearly, we apply a LEGION model with long-range horizontal connections to the medial axis points of segments to simulate the perceptual “pop-out” for well-aligned points and thus implement road segment grouping. Medial axis points, which are available from the previous stage, are considered as oscillators. Due to the one- dimensional nature of a medial axis, the orientation of each oscillator can be readily calculated from its neighborhood, and thus the connection strength can be computed based on the connectivity pattern.

Similar to applying LEGION to image segmentation, leaders are selected and stimulated for the sake of avoiding fragmentation. By LEGION dynamics, oscillators corresponding to the medial axis points of one road are synchronized while those corresponding to the medial axis points of different roads are desynchronized, and the oscillators that are not well aligned with any of the leaders can not be excited throughout the process, which completes the task of extracting roads and removing wrongly selected points.

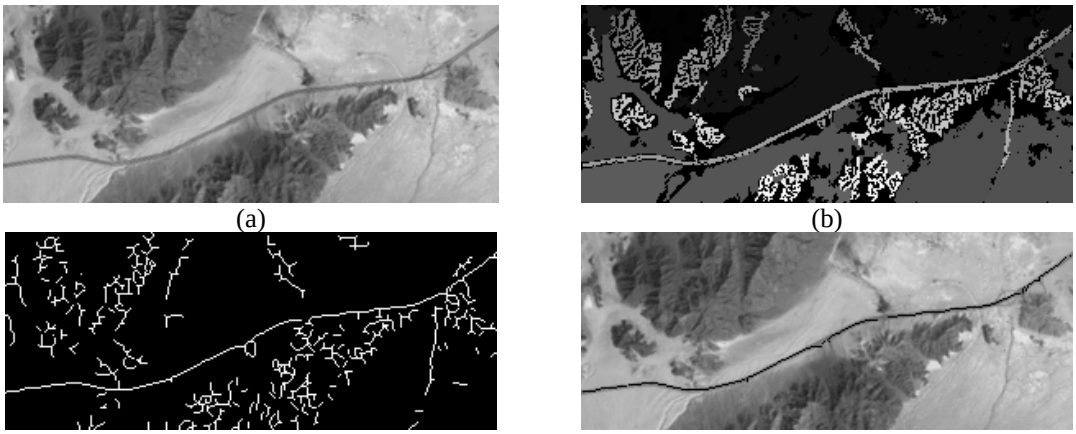

Figure 2. Results of road extraction from an image: (a) Satellite image containing a road (300 x 120 pixels), (b) The results of LEGION segmentation, (c) Candidate segments, and (d) Final results: extracted road (black line).

Figure 2 shows an example of the proposed method applied to satellite imagery. Figure 2a shows a subset of an IKONOS image collected over Baker, CA, with a resolution of 30 meters. This image contains a major road. Figure 2b shows the segmentation result, where each gray level indicates a distinct segment. The candidate medial axis points are then selected based on the segmentation result; these are shown in Figure 2c. The final result, shown in Figure 2d, is obtained by grouping the candidate points that form the road centerline. As can be seen, the road is clearly extracted.

REGION-BASED VECTOR GAC

In a RGB, multispectral or hyperspectral vector image, every pixel corresponds to a vector formed by pixel values from the multiple bands at the same pixel location; these vectors are referred to as pixel vectors. The Chan-Vese model has been extended to a vector version that takes an average of the image-fitting force (the force that drives the contours to fit image features) in all image bands (Chan and Vese, 2000). To handle hyperspectral images, we propose a variant model, which is referred to as Vector-GAC in this paper that adopts Euclidean distance in the image-fitting force.

Euclidean distance is a distance metric widely used in hyperspectral image processing (Keshava, 2004). Its definition is as follows. For two points, A and B, in an N-dimensional space, the Euclidean distance between A and B is:

$$E(A,B) = \sqrt{\sum_{k=1}^{N} (A_k - B_k)^2} \tag{1}$$

where A_k and B_k are the coordinates of the two points in the *k-th* dimension, respectively.

Letting I_i denote the intensity of the *i-th* band of an image with N bands in the domain Ω, ϕ denote the level set function which is a signed distance function, and C denote the contours represented as the zero level set of ϕ (i.e., $C = \{(x,y) \mid \phi(x,y) = 0\}$), we define the following energy function that is a variation and extension of the energy function proposed by Chan and Vese (Chan and Vese, 2000):

$$F(C,c_1,c_2) = \int_{inside(C)} \sqrt{\sum_{k=1}^{N} \left(I_k(x,y) - c_{k1}\right)^2}\, dxdy - \int_{outside(C)} \sqrt{\sum_{k=1}^{N} \left(I_k(x,y) - c_{k2}\right)^2}\, dxdy + \nu \cdot |C| \tag{2}$$

where c_{k1} and c_{k2} are the two constants that are the means of the image band I_k inside and outside the contours, respectively, $|C|$ represents the length of the contours, and ν is its coefficient. In this paper, the two vectors

$\vec{c}_1 = (c_{11}, c_{21}, \cdots, c_{N1})$ and $\vec{c}_2 = (c_{12}, c_{22}, \cdots, c_{N2})$ are referred to as target vectors. Compared with the energy function proposed by Chan and Vese (2000), the image-fitting force is composed of the Euclidean distances of a pixel vector to the target vectors rather than an average of the image-fitting force acquired in each band ($(I_k(x,y) - c_{k1})^2$ and $(I_k(x,y) - c_{k2})^2$).

The corresponding level set evolution function of the defined energy function given in Equation 2, which is the curve evolution function over time t, can be obtained (Chan and Vese, 2000):

$$\frac{\partial \phi}{\partial t} = \delta_\varepsilon(\phi)\left[\sqrt{\sum_{k=1}^{N}(I_k - c_{k1})^2} - \sqrt{\sum_{i=1}^{N}(I_k - c_{k2})^2} + \nu \cdot div\frac{\nabla \phi}{|\nabla \phi|}\right] \quad (3)$$

where δ_ε is the following approximated Delta function.

Equation 3 calculates the update of ϕ, and the curve evolution is achieved by calculating the update and applying it to ϕ iteratively. At a given pixel position in the image, the first two terms on the right side of Equation 3, which are the image-fitting terms, calculate the Euclidean distances between a pixel vector and the two vectors $\vec{c}_1 = (c_{11}, c_{21}, \cdots, c_{N1})$ and $\vec{c}_2 = (c_{12}, c_{22}, \cdots, c_{N2})$, which are referred to as the target vectors in this paper. The vectors $\vec{c}_1$ and $\vec{c}_2$ are self-adaptive and keep being updated during the contour evolution. The third term, which is the curvature term, controls the smoothness of the contours and suppresses noise with the stretching force (Kass et al., 1987). The function δ_ε constrains the evolution update of ϕ happening in a narrow band of the current contours.

The two-phase vector-versioned active-contour model represented by Equation 3 intuitively acts as a hyperplane to divide a data cloud generated from a vector image into two clusters based on Euclidean distance. This corresponds to separating the image into the foreground (pixels inside the contours) and the background (pixels outside the contours); the smoothness of the boundaries of these two areas is controlled by the curvature term.

Figure 3 shows an example of this two-phase segmentation through use of Equation 3 on a synthetic RGB image. The original image contains noise and has four classes of objects based on the colors red, green, dark gray and light gray. Given the initial contours as shown in Figure 3b, the contours shown in Figure 3d were obtained by the curve evolution; the two-phase segmentation results are shown in Figure 3e. It can be seen that noise was removed and segments with smoothed boundaries were acquired.

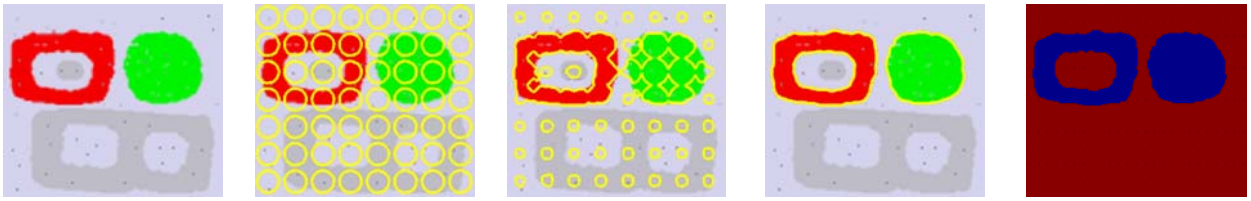

(a) (b) (c) (d) (e)

Figure 3. Example of the two-phase segmentation with Equation 3 dividing the image domain into two subregions (foreground and background). The contours are shown in yellow. (a) Original RGB image, (b) Initial state of contour evolution with automatically generated initial contours, (c) A median state of curve evolution (d) Final state of contour evolution, and (e) Two-phase segmentation results (each color represent one class).

The multi-phase approach is needed to classify an image with more than two classes of objects rather than separating it into foreground and background. Two approaches are usually used to extend the two-phase model to a multi-phase model. One is to have more than one level set function to represent multiple classes and use rules to prohibit vacuum and overlap (Samson et al. 2000; Brox and Weickert, 2004). The other is to allow further separations in the subregions of the image acquired in previous segmentations and sequentially segment different classes in a hierarchical manner (Tsai, 2001; Ball and Bruce, 2005). As the first approach requires some prior knowledge such as the number of classes in the image, the second approach was selected in our research;. This approach corresponds to a coarse-to-fine classification strategy and enables users to have better control of the classification procedure.

The idea behind this multi-phase active contour approach is to apply the two-phase model recursively on each of the two subregions obtained in the upper level (if any of them require further separations). On the top level, the whole image domain is set as the working domain for curve evolution, and the corresponding subregions are set as the working domain in lower levels. The example shown in Figure 4 separates the image into four classes in two levels of two-phase segmentations. The nonblack area represents the working domain in the current level. The implementation procedure of this method is similar to a binary split tree, as illustrated in Figure 4. The number of recursion levels (layer of the binary split tree) determines the maximum number of classes that can be extracted, which is the square of the number of recursion levels.

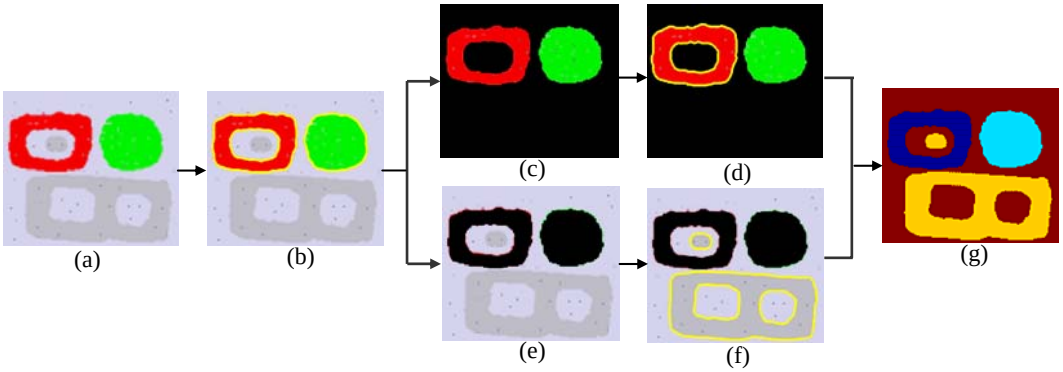

Figure 4. Example of multi-phase segmentation (classification) of a synthetic RGB image. The contours are shown as yellow lines, and the nonworking domains are shown in black. The initial contours in this example were automatically generated in the same way as those generated in the example shown in Figure 1. (a) Original image with initial contours, (b) Level 1 segmentation (separate the original image into two subregions), (c) Subregion I, (d) Level 2 segmentation of subregion I that is further separated into two subregions, (e) Subregion II, (f) Level 2 segmentation of subregion II, and (g) Classification results with four classes (each color represents one class).

EXPERIMENTS

Preliminary experiments on target extraction from multiple-source imageries using the algorithms described in the two sections above were performed on EO-1 Hyperion hyperspectral and IKONOS multispectral images collected at Silver Lake, California. The EO-1 Hyperion imagery has 30-m resolution and is a Level 1GST product. It was acquired in October 2003. The image size selected for the experimental area is 140 x 140 pixels. The original dataset had 242 bands ranging from 447.17 nm to 2577.08 nm; 156 bands were left after removal of bands with unconstructed noises. The IKONOS multispectral imagery was collected in October 2008. It has four bands (red, blue, green and infrared), and its resolution is 4 m. The experimental datasets of the two imageries are shown in Figure 5.

(a) (b)

Figure 5. The image datasets used in the experiment. (a) RGB color image of three selected EO-1 Hyperion images, image size: 140 x 140. (b) Pseudo-color (R, N, G) image of the IKONOS dataset, image size: 693 x 516.

Figure 6 outlines the workflow. First, EO-1 Hyperion hyperspectral imagery with 30-m resolution is reduced to a low number (8) of dimensions via dimensionality reduction method of LTSA (Local Tangent Space Alignment, Zhang et al., 2004; Zhou et al., 2009). Then, Vector GAC is applied to classify the images and obtain the candidate targets. After this, the LEGION-based road-extraction algorithm is used to extract road segments based on the segments of the candidate targets. Subsequently, the candidate segments are projected onto 4-meter-resolution IKONOS multispectral imagery, and are used as prior knowledge to help the Vector GAC model extract targets with refined boundaries.

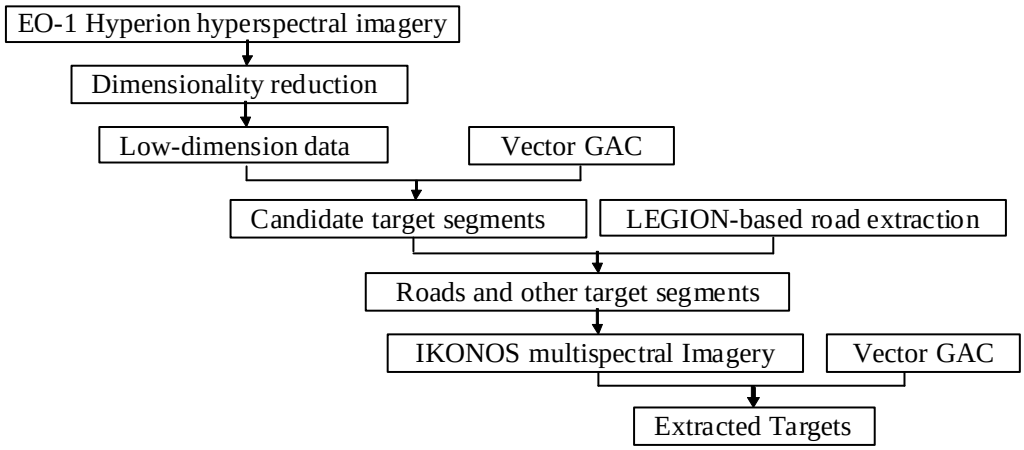

Figure 6. Workflow of target extraction from multiple-source imagery.

The segments of the classes obtained on the EO-1 dataset were to be mapped onto the IKONOS imagery. As some classes are distinguished from each other on this 30-m-resolution imagery only because of different levels of mixture (mainly with the background) and they actually contain the same types of objects, each of the following two class pairs were merged into one class before we turned to the 4-m-resolution IKONOS imagery on which the mixture is far less important: *vegetation A* and *vegetation B*, and *low-moisture soil* and *high-moisture soil*. The two

classes *asphalt surface A* and *asphalt surface B* show different spectral characteristics on EO-1 imagery that are not caused by the mixture issue. The visible and infrared bands on EO-1 imagery also reflect this difference, but this was not observed on the IKONOS imagery with R, G, B and infrared bands. So they were also merged into one class.

After the classified segments obtained on low-resolution images were mapped onto the high-resolution images, it is desirable to constrain the search area within the area marked by the mapped segments when performing target extraction on the high-resolution images. However, the dimensions of the targets should be taken into account as relatively smaller targets can be missed (classified as background) or classified into other classes on the low-resolution images due to the mixture issue. When this happens, any area where this type of target is not mapped cannot be excluded from the search area on the high-resolution imageries. This is the case for all the classes obtained on the EO-1 imagery, which has a resolution of 30 m.

After the segments of the regrouped classes (*vegetation*, *asphalt surface*, *soil moisture* and *main roads*) were mapped onto the IKONOS imagery, the boundaries of the mapped segments were taken as the initial contour for the Vector GAC, which then extracted the targets of these classes sequentially. The building objects (shown in white in Figure 5 in both the EO-1 and IKONOS images) were not represented in any of the DR bands of the EO-1 imagery and, as a result, they were not obtained by the classification on the eight DR bands. Therefore, before the extraction of other targets, the building objects were extracted by Vector GAC whose initial contours were provided by obtaining the pixels whose intensity is larger than a certain threshold. Each time the objects of one class (including buildings) were extracted, the corresponding segments were excluded in the working domain of Vector GAC. In other words, the extraction of other targets was performed only in the remaining domain of the image. The final target extraction results are shown in Figure 8.

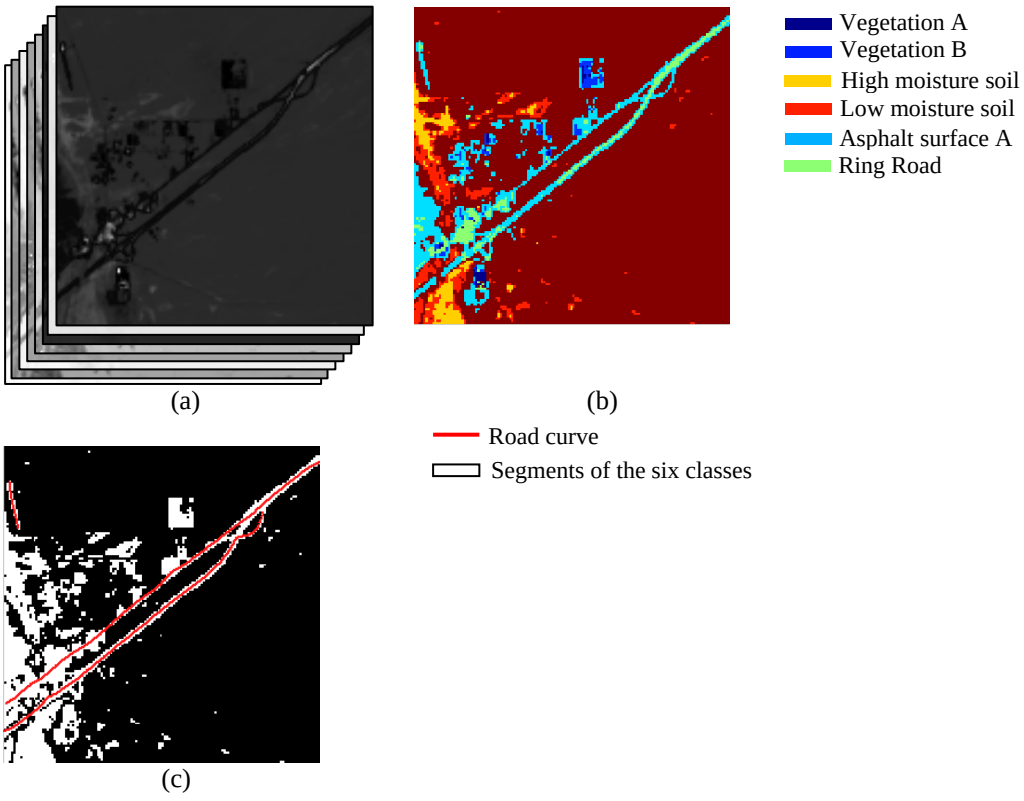

Figure 7. Illustration of the Vector GAC model on EO-1 hyperspectral imagery: (a) Dimensionality reduced imagery (156 reduced to 8 bands), (b) Classification results by Vector GAC, and (c) Extracted road curves on the segments of the classes in (b) by the LEGION-based road-extraction.

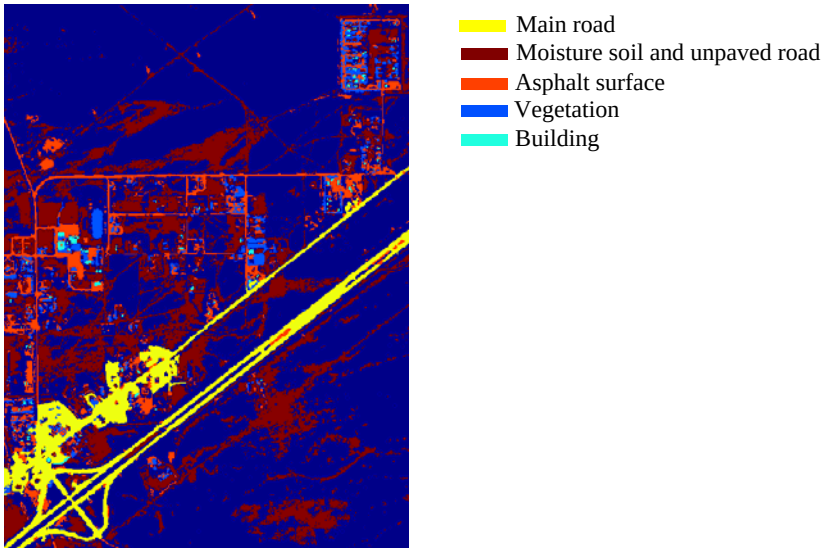

Figure 8. Target extraction results from IKONOS multispectral imagery.

The above-described experiments have shown that information obtained from the low-resolution imagery can be used as prior knowledge for the processing of high-resolution imagery. In this case, the classification and road extraction results obtained from the EO-1 Hyperion imagery were used to provide initial contours for the Vector GAC model to perform target extraction on the IKONOS imagery.

The experimental results also indicate that the characteristics of both the processing methods and the image sources must be considered when selecting the image processing methods for different image datasets. For example, Vector GAC is appropriate for the 4-m-resolution IKONOS multispectral imagery as it has the ability to provide smooth boundaries and suppress noise where the boundaries of the man-made objects are relatively clearly reflected. However, it is not the ideal choice for EO-1 imagery, and in future work it will be replaced by Spatial-LEGION, a vector version of LEGION. There are two reasons why the Vector GAC is inappropriate to be applied on EO-1 Hyperion images. For one thing, on this 30-m-resolution imagery, smooth boundaries for the targets cannot be expected because of the relatively small dimensions of the targets when compared to the resolution of the dataset. Also, the noisy pixels could actually be the target of interest and therefore should not be suppressed. Thus in this experiment, when Vector GAC was applied to the EO-1 imagery the coefficient of the curvature term in Equation 3 was tuned to 0 such that the Vector GAC degraded to a Euclidean distance-based classifier and there was no boundary regulation and noise suppression provided by it. Also, Vector GAC uses Euclidean distance as the distance metric, which is similar to taking an average of the image intensity differences among all input image bands. If a type of target is represented in only one or a few input bands, it is possible that the difference of this target feature from other targets is not well represented by the Euclidean distance, and thus is classified incorrectly such as the unpaved roads that were classified as background on the EO-1 Hyperion imagery. Therefore, although the results shown in Figure 6b look reasonable, the possibility exists that some targets were missed, and the use of Spatial-LEGION, which adopts an appropriate distance metric to be able to detect details that appear in only a small number of bands, can be expected to generate better results.

An initial DR study was carried out in (Wu et al, 2009; Zhou et al., 2009). The issue of possible data loss in DR needs to be further considered as well. As shown in Figures 5a, some building objects are visible only in a particular spectral range (mainly in the visible bands) of the EO-1 imagery, but they are not represented in the DR results of LTSA. This reveals the risk of losing information in the DR process, and further testing of these DR methods are needed including other non-linear DR techniques of LLE (Local Linear Embedding. Roweis, 2000; Han and Goodenough, 2005) and LE (Laplacian Eigenmap, Belkin and Niyogi, 2003) and the linear DR techniques of PCA and MNF (so far none of these methods were able to generate DR bands able to distinguish building objects from the asphalt surface on the 156 bands).

CONCLUSIONS

We have developed algorithms for the LEGION-based road extraction and the Vector GAC methods, and have applied them to multiple-source remote-sensing imageries that include EO-1 Hyperion hyperspectral and IKONOS multispectral images for target extraction. The experimental results show that the information obtained from the low-resolution imageries can be used as the prior knowledge to improve the processing of the high-resolution images, reducing computation complexity and, in particular, making it possible to distinguish main roads from other asphalt surfaces that are spectrally indistinguishable. Improvements on LEGION and GAC will be made in the future work to better fit the characteristics of the imageries on which these algorithms are applied. The research will also be made on DR, and supervision techniques will be considered either in the process of the DR or in the selection of spectral range of the input bands for DR.

ACKNOWLEDGEMENTS

This research is funded by the NGA University Research Initiatives program.

REFERENCES

Ball, John Eugene and L. M. Bruce, 2005. Level set segmentation of remotely sensed hyperspectral images, *Proceeding of IGARSS*, 8: 5638–5642.

Belkin, M., and P. Niyogi, 2003. Laplacian eigenmaps for dimensionality reduction and data representation, *Neural Computation*, 15(6):1373-1396.

Brox, Thomas, and J. Weickert, 2004. Level set based image segmentation with multiple regions, in *Pattern Recognition, Rasmussen*, C.-E., Bulthoff, H., Giese, M. and Scholkopf, B. (Eds.), Springer.

Caselles, Vicent, F. Catte, T. Coll and F. Dibos, 1993. A geometric model for active contours in image processing, *Numerische Mathematik*, 66(1):1–31

Chan, Tony, Y. B. Sandberg, and L. Vese, 2000. Active contours without edges for vector-valued Imageimage, *Journal of Visual Communication and Image Representation*, 11(2): 130–141.

Chan, Tony and L. Vese, 2001. Active contours without edges, *IEEE Trans. Image Processing*, 10(2):266–277.

Field, David J., A. Hayes, and R. F. Hess, 1993. Contour integration by the human visual system: Evidence for a local 'Association Field', *Vision Research*, 33(2):173–193.

Han, T., and D.G. Goodenough, 2005. Nonlinear feature extraction of hyperspectral data based on locally linear embedding (LLE), *Proceedings of 2005 Geoscience and Remote Sensing Symposium*, 2:1237-1240

Kass, Michael, A. Witkin, and D. Terzopoulos, 1987. Snakes - active contour models, *International Journal of Computer Vision*, 1(4): 321–331.

Keshava, Nirmal, 2004. Distance metrics and band selection in hyperspectral processing with applications to material identification and spectral libraries, *IEEE Trans.Geosci. Remote Sens.*, 42(7): 1552-1565.

Niu, X., 2006. A semi-automatic framework for highway extraction and vehicle detection based on a geometric deformable model, *ISPRS Journal of Photogrammetry and Remote Sensing*, 61(3-4):170-186.

Roweis, S.T., 2000. Nonlinear dimensionality reduction by locally linear embedding, *Science*, 290(5500):2323-2326.

Samson, Christophe, L. Blanc-Fraud, G. Aubert, and J. Zerubia, 2000. A level set model for image classification, *IJCV*, 40(3):187–197.

Terman, David, and D.L. Wang, 1995. Global competition and local cooperation in a network of neural oscillators, *Physica D*, 81: 148-176.

Tsai, Andy, A. Yezzi Jr., and A. S. Willsky, 2001. Curve evolution implementation of the Mumford-Shah functional for image segmentation, denoising, interpolation, and magnification, *IEEE Trans. Image Processing*, 10(8): 1169–1186.

Wang, Deliang, and D. Terman, 1997. Image segmentation based on oscillatory correlation, *Neural Computation*, 9: 805-836.

Wang, DeLiang, 2005. The time dimension for scene analysis, *IEEE Transactions on Neural Networks*, 16: 1401-1426.

Wu, Bo, Y. Zhou, L. Yan, J. Yuan, D.L. Wang, R. Li, 2009. Object detectionfrom HS/MS and multi-platform remote sensing imagery by integration of biologically and geometrically inspired approaches, *Proceedings of ASPRS 2009 Annual Conference*, Baltimore, Maryland, March, 2009.

Yen, Shih-cheng and L. H. Finkel, 1998. Extraction of perceptually salient contours by striate cortical networks, *Vision Research*,. 38(5): 719–741.

Zhang, Z., and H. Zha, 2004. Principal manifolds and nonlinear dimensionality reduction via local tangent space alignment, *SIAM journal of Scientific Computing*, 26(1): 313-338.

Zhou, Yuan, B. Wu, D. Li and R. Li, 2009. Edge detection on hyperspectral imagery via manifold techniques, *Hyperspectral Image and Signal Processing: Evolution in Remote Sensing*, WHISPERS '09.